An Investigation of Electro-Hydraulic High Efficient Power Package Configurations for a More Electric Aircraft System Architecture

N. Trochelmann, T. Rave, F. Thielecke
Hamburg University of Technology, Institute of Aircraft Systems Engineering
Neßpriel 5, 21129 Hamburg, Germany

D. Metzler
Liebherr-Aerospace Lindenberg GmbH,
Pfänderstraße 50-52, 88161 Lindenberg/Allgäu, Germany

ABSTRACT

The trend for optimized electric secondary power generation and distribution systems in commercial aircraft requires electric actuation technology. Electro-hydraulic systems with electric motor-driven pumps (EMP) will likely serve as bridge technology for several actuation functions in the medium- (or long-) term. They enable to apply dissimilar actuation technologies in critical applications or where intrinsic advantages of hydraulic actuation shall be kept. Following the general design requirements for more electric aircraft (MEA) systems, like higher efficiency, lower cost, easier maintenance, and quicker installation, this study investigates the application of electro-hydraulic high efficient power packages (eHEPP) as electro-hydraulic supply modules. The eHEPP integrates the hydraulic system components and the EMP in a compact line replaceable unit. A variable speed EMP concept is applied to achieve a high efficiency of the eHEPP. Under the assumption that landing gear and empennage flight control actuation is hydraulic, different system configurations, ranging from a centralized system with one main eHEPP to a distributed system with local eHEPPs, are designed. In order to find the best concept the key performance of these configurations is evaluated according to the criteria system mass, reliability, availability and efficiency. The evaluation is based on a steady state system sizing and preliminary safety studies. A typical short range aircraft, similar to the Airbus A320 or the Boeing 737, serves as reference for geometry and flight control concept. The study was performed in cooperation with Liebherr-Aerospace Lindenberg GmbH as part of its contribution to the Clean Sky 2 Systems ITD.

1. INTRODUCTION

Full electric secondary power generation and distribution systems are one of the major goals in civil aircraft industry. A main advantage is an optimized use of secondary power generation enabled by an overall and flexible electric power management [1]. Furthermore, a full electric distribution system allows for easier fault isolation and reconfiguration of power paths [2]. An improved dispatch reliability of the aircraft is expected as the number of hydraulic components and thus potential leakage sources are reduced [3]. Large and heavy engine driven pump (EDP) suction lines can be eliminated [4]. However, a full electric system can only be achieved, if reliable and mature electric actuation technology is available. This need and the advancements in the field of electric drives and control [1] have triggered the development of different Power by Wire (PbW) actuation concepts. The two main candidates are electro-mechanical (EMA) and electro-hydrostatic actuators (EHA). Both concepts still come along with major challenges and specific drawbacks. For EMA jamming is a major issue and its reliable prediction

is not possible so far because it requires years of flight experience [5]. Unlike EMA the EHA technology has already entered into service in primary flight control applications aboard the Airbus A350 and A380. Though, EHAs (and hybrid forms) are mostly operated in stand-by mode and only become active in the event of a failure in the conventional hydraulic lanes [6]. Technical challenges of the EHA are heat rejection and reliability in frontline operating mode.

Due to uncertain, respectively lacking reliability and maturity of the PbW actuation concepts a full electrification of the aircraft actuation functions appears unlikely in medium- (or long-) term. More electric aircraft (MEA) system architectures with different partial electrification concepts are subject of several research activities. This publication focusses one particular concept of a MEA system architecture. Specifically, the idea of an electric wing (E-Wing) complemented by an electro-hydraulic (eH) system for empennage flight controls (F/C) and the landing gear, as shown in FIGURE 1, is considered. The eH system is supplied by electric motor-driven pumps (EMP) and allows to retain ordinary and proven

hydraulic actuators [7] in cases where the intrinsic advantages of hydraulic actuation shall be kept (landing gear) or where reliable and dissimilar actuation technology is needed, to lower the technical risk of full PbW actuation (empennage F/C). A recent example for the concept of an eH system is the centralized eH system in the Boeing 787. It is supplied from two large EMPs [4] making the hydraulic system an electric consumer.

This study investigates the application of electro-hydraulic high efficient power packages (eHEPP) as supply units of an eH system with essential actuation functions. The integrated concept of an eHEPP strives for a reduction of the hydraulic installation time, which is a major disadvantage of conventional hydraulic systems. The design of an eHEPP is challenging since there is a wide range of potential configuration options. Depending on the number and type of allocated consumers the eHEPP configuration can either be distributed with local eHEPPs, as illustrated in FIGURE 1, or centralized with one main eHEPP. The objective of this publication is to find the optimal eHEPP system configuration as the best compromise between the design drivers system mass, efficiency, availability, and reliability.
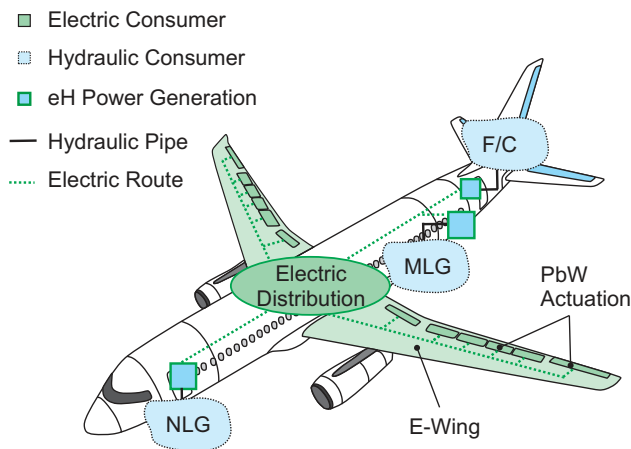

FIGURE 1: MEA System Concept with E-Wing and eH-System for Essential Functions

The study starts out with the definition of the specific baseline MEA system architecture with E-Wing actuation concept. Further, this includes the specification of the hydraulic functions that have to be covered by an eHEPP. Based on that, different eHEPP configurations with varying allocations of consumers and numbers of eHEPPs are developed followed by the conceptual design of the eHEPP and its components. Via a steady state system sizing and safety analyses the performance of the eHEPP configurations is evaluated in order to find the best concept.

2. BASELINE SYSTEM ARCHITECTURE

By making use of the advantages of a central electric distribution and by keeping the proven hydraulic actuation in cases where PbW actuation appears disadvantageous or challenging, a 2E1eH overall system architecture is defined as framework for this study. The proposed 2E1eH architecture is shown in FIGURE 2. It is formed by two central electric systems and one eH system supplied by the eHEPP(s). The configuration of the eH system is variable and is detailed in this study. Compared to the conventional 3H or 2H1eH architectures two main electric systems replace two central hydraulic systems with EDPs. A typical short range aircraft, similar to the Airbus A320 or the Boeing 737, serves as reference for the flight control concept and geometry.
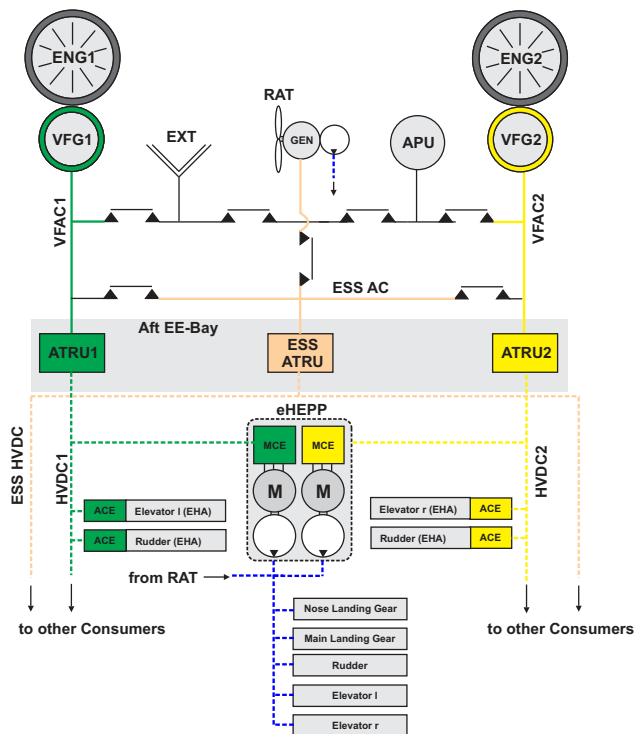

FIGURE 2: Baseline System Architecture 2E1eH (with Central eHEPP Configuration)

2.1. Electric Generation and Distribution System

The electric power sources are two variable frequency generators VFG1 and VFG2 that are driven by the engines. The VFGs feed the power into the variable frequency alternating current (VFAC) buses VFAC1 and VFAC2. This concept is adapted from modern aircraft like Airbus 380 and Boeing 787, which are using variable frequency systems instead of a traditional 400 Hz/115 VAC network with constant frequency. This allows to eliminate the heavy, complex, and maintenance-intensive constant speed drive. In

modern aircraft a clear step to higher AC voltage levels can be observed. Higher voltage levels reduce currents in the transmission line so that cable cross sections can be downsized and weight can be saved. Moreover, high voltage direct current (HVDC) power networks offer an additional advantage over AC systems: the elimination of the skin effect, which enables further downsizing of cable cross sections. Hence, in the baseline architecture two central ATRUs convert the VFAC power to HVDC power that is distributed via the buses HVDC1 and HVDC2, similar to [8]. For simplicity central HVDC grids without isolated HVDC systems for F/C are assumed. Emergency power is provided by the ram air turbine (RAT). The RAT has either a hybrid design with a generator for essential electrical functions and a pump for hydraulic back-up power or a purely electric design. The RAT generator supplies the essential AC bus (AC ESS) while the RAT pump supplies flow to the eH system.

2.2. E-Wing Actuation Concept

As illustrated in FIGURE 1, the E-Wing concept abandons conventional hydraulic actuation and distribution system from the wing. Instead PbW actuation technology is applied. In the wing aileron and spoiler form redunant surfaces for roll control so that the failure of single control surfaces has less severe impacts on aircraft level compared to the empennage surfaces. For instance, a jammed EMA could be oversteered by a redundant control surface. However, it is not further discussed in this article, whether EMA or EHA (or hybrid) technology should be applied. The E-Wing concept also envisages electric actuation of the high-lift functions by an electrical power control unit (PCU). Examples for the replacement of hydraulic motors by electric motors are the hybrid PCUs for slat actuation of the Airbus A350, Boeing 777, and Boeing 787. Full electric PCUs can be found in Sukhoi Superjet 100 or Embraer E-Jet. Similarly, electrical actuation of the trimmable horizontal stabilizer actuator is considered.

2.3. Hydraulic Consumers

The immediate realization of a full PbW actuation concept in the empennage appears unlikely in the considered concept because pitch and yaw control (left and right elevator and rudder) have no redundancies. Jamming of an EMA would be a severe issue and EHAs have not yet proven their reliability in front line operation. For this reason it is assumed that the empennage flight controls use jam-free, conventional hydraulic servo control units (SCUs). Since there is only one hydraulic system, additional EHAs are applied to build up the required redundancy. Moreover, using dissimilar actuator technologies in this essential application increases the functional safety. It is worth mentioning that a similar concept for the supply of empennage F/C via a hydraulic power package was investigated and demonstrated experimentally in [9].

For landing gear electro-mechanical actuation has several drawbacks compared to conventional hydraulic actuation. While it appears feasible to implement electro-mechanical extension and retraction, the realization of secondary functions with EMAs, like braking, steering, door actuation, locking, freefall and self-alignment make landing gear with EMAs heavier and more complex [10]. Hydraulic solutions for these functions require less effort. For instance the freefall function is implemented by opening a valve with an orifice. Similarly, the declutching of the steering is realized by a by-pass in the valve. Thus, a hydraulic actuation concept for the landing gear is considered in this study. The decision is also supported by promising research projects on eH actuation concepts for a main landing gear (MLG) in [11] and a nose landing gear (NLG) in [12] and [13].

2.4. Design of eHEPP-Configurations

Dependent on the allocation of the described hydraulic consumers to eHEPP(s), the design options vary from one large, central eHEPP supplying all functions to a distributed configuration with multiple eHEPPs for local supply. The design space is limited by the following assumptions:

- The empennage F/C are supplied by the same eHEPP.

- The functions of the MLG (extension, retraction, door actuation) are supplied by the same eHEPP. Braking is assumed to be electric.

- The NLG functions (extension, retraction, steering, door actuation) are supplied by the same eHEPP.

This results in three groups of consumers: (empennage) F/C, MLG, and NLG. The allocation of these consumers to the eHEPP(s) yields the four eHEPP configurations that are shown in TABLE 1. Configuration A, which represents a distributed eHEPP system, and configuration C, a central eHEPP system, form the extremes of the design space. In the following these two configurations are detailed.

TABLE 1: eHEPP Consumer Allocation

Confi-guration	NLG	MLG	F/C
A	eHEPP1-A	eHEPP2-A	eHEPP3-A
B	eHEPP1-B		eHEPP2-B
C	eHEPP1-C		
D	eHEPP1-D	eHEPP2-D	

2.4.1.   Distributed Configuration (A)

The distributed eHEPP configuration A, respectively its topology is illustrated in FIGURE 3. It shows the installation locations of the consumers, of the eHEPPs, and of the ATRUs. Moreover, it defines the assumed routing of pipes and power cables (communication cables and computers are not illustrated), which are determined by the installation locations of the eHEPPs and of the allocated consumers.
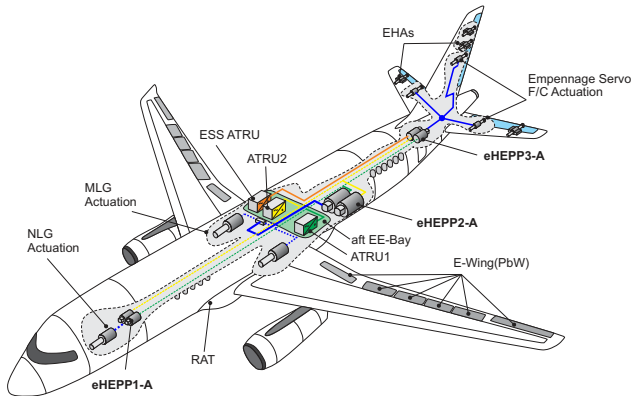

FIGURE 3: Distributed eHEPP Configuration

Configuration A features three independent hydraulic (sub-) systems. The functions of the NLG are supplied by eHEPP1-A. It is assumed to be installed in the wheel well of the NLG so that pipe work between eHEPP1-A and NLG is short. The concept of a local hydraulic supply of the NLG is under investigation in a parallel Clean Sky Project in Systems ITD [13]. The position of eHEPP2-A is defined to be in the aft belly fairing. The location of the MLG consumer is represented by the MLG valve manifold. The MLG pipe line considered in the comparative study ends at the manifold because the pipe work downstream is identical in each eHEPP configuration. The location of eHEPP3-A in the empennage is behind the bulkhead. All hydraulic lines are assumed to run along structure elements like frames, spars or ribs.

Each eHEPP needs supply of 28 VDC for control and monitoring voltage and 540 VDC (HVDC) for the power drive electronics. Note that a redundant eHEPP needs redundant supply. The central ATRUs are assumed to be located in a central power center in the aft EE-Bay. Also the TRUs for generation of 28VDC (not illustrated) are located in the aft EE-Bay. For the calculation of the induced electric mass only parts of the electric system that are required for the supply of the specific eHEPP (solid lines) are considered:

- The electric generation system (generator, TRU, ATRU) is identical for the different concepts. The impact of different eHEPP configurations on its sizing is neglected.

- The EHAs in the empennage are supplied by HVDC1 and HVDC2 and by 28VDC so that these power lines can also be used to supply eHEPP3-A (dashed lines).

Hence the induced electric mass in configuration A is mainly determined by the power supply lines from the aft EE Bay to eHEPP1-A and eHEPP2-A. It has to be noted that the empennage eHEPP3-A supplies safety critical flight control actuators and requires therefore the connection to the RAT. For the RAT, located forward of the wing, an electric RAT (E-RAT) is chosen for configuration A to avoid an additional long hydraulic pipe line. Hence, the extra power cable for a connection of eHEPP3-A to the ESS HVDC bus (see FIGURE 2) is considered in the mass calculation.

The eHEPP and the flight control computers are connected via the avionics fully duplex switched Ethernet (AFDX) network. The relevant flight control computers are assumed to be located in the forward EE-Bay below the cockpit directly at the NLG. For the eHEPP bus communication a central AFDX route from the forward EE-Bay to the empennage is assumed. Since the connection between eHEPP1 and the computers is assumed to be short it is neglected. As a result only the central route and the branchings to eHEPP2 are considered in the AFDX mass evaluation.

2.4.2.   Central Configuration (C)

The design of the central eHEPP configuration C is illustrated in FIGURE 4. It represents a central hydraulic system with one central eHEPP1-C that supplies all consumers. It is similar to the central Boeing 787 eH system that also supplies the landing gear. The central eHEPP is assumed to be located in the same position as eHEPP2-A.
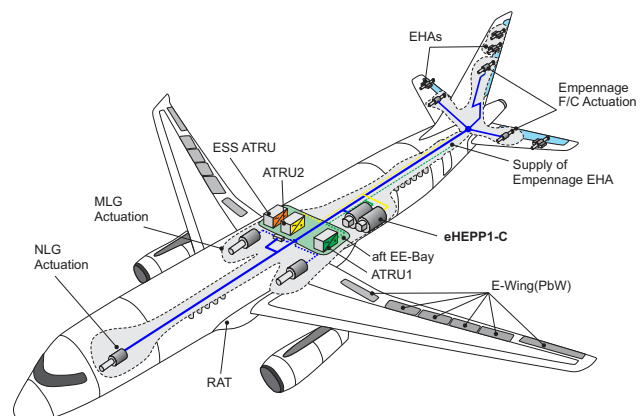

FIGURE 4: Central eHEPP Configuration

The described locations of consumers, EE-bays and flight control computers are the same as for configuration A so that only differences in the routings of

pipes, cables and AFDX buses are described. The central pipe system is assumed to run from the front to the back of the aircraft, in the center of the fuselage. Here, a hybrid RAT appears advantageous because the RAT pump could be connected via a short extra pipe to the central system, see FIGURE 2. For the power supply of the eHEPP only the short branches from the main HVDC and 28VDC lines need to be considered. Similarly, for the communication only the (additional) routing of the AFDX bus system from the forward EE-Bay to eHEPP1-C is taken into account.

3. eHEPP SYSTEM AND COMPONENTS

Primary design drivers for the eHEPP are low weight and high efficiency. Furthermore, aircraft manufacturers intend to reduce (hydraulic) installation times at the final assembly line (FAL) to enable higher production rates. Besides, the eHEPP must represent a system with high reliability and operational availability.

3.1. Electric Motor-Driven Pump

The key to a high efficient power supply is an innovative concept for the EMP. The conventional EMP design, formed by a variable displacement axial piston pump (AKP) and an asynchronous motor (ASM), has served for decades. It is robust and proven but it has significant drawbacks:

- The volumetric losses of the AKP cause a poor part load efficiency. This means significant power losses because the system is operated at part load most of the time (see FIGURE 7).

- The EMP is operated at constant, high speed causing high noise as well as speed induced wear and power losses.

- The ASM is typically connected directly to the $400\,\mathrm{Hz}/115\,\mathrm{V}$ AC system (without regulating power electronics). In a MEA with VFAC (or HVDC) grids the direct connection would be difficult and may lead to an oversizing of the EMP [14].

As DUNKER points out in [14], usage of frequency inverters is necessary in a MEA electric power system. This also allows to use speed controlled drives, like permanent magnet synchronous motors (PMSM), and it enables alternative EMP concepts with variable speed and fixed (VSFD) or variable displacement. EMP concepts with variable speed were investigated in detail for general/industrial hydraulic applications in [15] and [16], revealing a great potential of energy saving. Based on these results DUNKER designed and demonstrated the concept of a VSFD EMP with an internal gear pump (IGP) in [14] and showed a great noise reduction potential and a high part load efficiency, which makes this EMP concept

well suited for the typical duty cycles in aircraft hydraulic systems. FIGURE 5 compares the efficiencies of the VSFD EMP concept to the conventional EMP.
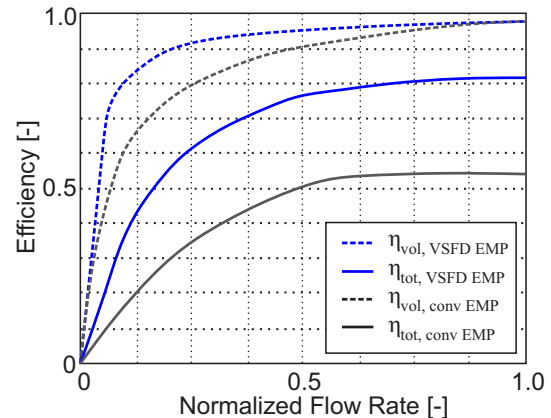
FIGURE 5: Comparison of Efficiencies of Conventional and VSFD EMP Concept [14]

As the VSFD EMP concept promises an efficient operation it is considered in this study. Owing to the goal of a light eHEPP a high maximum EMP speed of $10,000\,1/\mathrm{min}$ is specified. This allows a smaller sizing of the pump's displacement volume and that in turn lowers the required driving torque of the motor. The EMP is pressure controlled, providing a conventional constant pressure level of $3000\,\mathrm{PSI}\ (206\,\mathrm{bar})$ over the entire flow range.

3.2. eHEPP System Design

The eHEPP system design follows the approach of a line replaceable unit (LRU). The interfaces between the eHEPP LRU and aircraft are the electric connector of the MCE, an AFDX connector for communication, and the hydraulic ports. The hydraulic power generation is the main function of the eHEPP and is realized with a VSFD EMP as described previously. The electric power is modulated via a dedicated motor control electronic (MCE). The MCE does not necessarily have to be integrated in the package so that it could be placed in the pressurized and conditioned area in order to improve reliability [3].

For fluid storage a bootstrap reservoir is used since pneumatic pressure may not be available. All common hydraulic system components like filters, accumulator, valves, and sensors are mounted to the high pressure manifold. Furthermore, extra cooling for the motor and the MCE needs to be considered. The cooling of the PMSM is realized by a hydraulic jacket cooling using the return oil while the MCE cooling concept depends on the installation location. Specifically, on the availability of a liquid cooling circuit. An eHEPP located in the tail is assumed to be cooled with air while an eHEPP located close to the
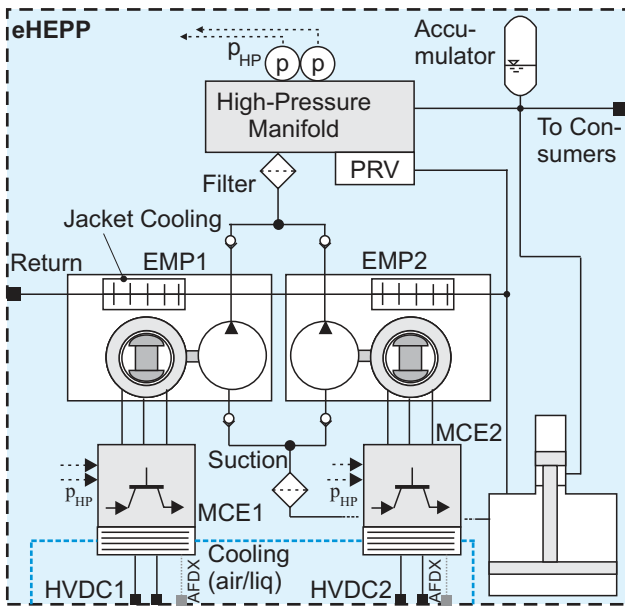
FIGURE 6: eHEPP System Concept with Redundant EMPs and MCEs

aft EE-Bay is assumed to be using the cooling system of the aft EE-Bay or common fuel heat exchanger.

The eHEPP must provide a high availability by ensuring a failure probability of $F_{eHEPP} < 1 \cdot 10^{-5}$ /FH. Based on the mean time between unscheduled removal (MTBUR) rates of the components the achievable availability of different redundancy concepts (e.g. two motors, two pumps etc.) were evaluated applying the reliability block diagram (RBD) techniques (see [17]). It was shown that only a design with two redundant EMP units, as shown in FIGURE 6, can meet the required availability. Hence the redundant eHEPP design serves as baseline for the subsequent system sizing.

4. SYSTEM KEY PERFORMANCE ESTIMATION

The comparative evaluation of the eHEPP configurations is based on the following key performance indicators (KPI): system complexity and availability, system mass, and power consumption. Furthermore, the system safety is investigated for all configurations to ensure their feasibility.

4.1. Safety, Complexity and Availability

System Safety
For the evaluation of the system safety a preliminary system safety analysis (PSSA) is conducted. The following top level events regarding the primary flight controls are considered:

- loss of elevator control,
- loss of rudder control, and

- loss of rudder control and loss of one engine.

All events are classified to be catastrophic and must be extremely improbable with the safety target of $F \leq 1 \cdot 10^{-9}$ /FH. The three top events are considered in separate PSSAs. It is assumed here that the loss of the landing gear does not affect the overall eHEPP system safety and that the reliability of the hydraulic pipe system is independent of its length, so that the configurations A through D have the same reliability F (failure probability)

(1) $\quad F_A = F_B = F_C = F_D = F.$

The determination of the failure probability F is described in the following using the example loss of rudder control. The system is modeled with RBDs formed by three critical (minimal) paths:

- **Path1:** Electric Supply - HVDC1 - EHA 1,

- **Path2:** Electric Supply - HVDC2 - EHA 2,

- **Path3:** Electric Supply - HVDC1 & HVDC2 - eHEPP - SCU

Only the simultaneous failing of all three paths leads to the loss of rudder control. All paths contain the critical sub-event loss of the electric supply. The electric power supply in turn has three redundant paths, two engine paths [ENG1, VFG1, VFAC; ENG2, VFG2, VFAC] and the APU path [APU, APU GEN, VFAC]. Only in case that all three generation paths or the ATRUs are lost, normal electric power supply is not available for the eHEPP and the EHAs anymore. Then, emergency power will be supplied from the RAT. It has to be noted that the impact of the flight control computers is neglected but has to be included in future studies.

System Complexity
In general the complexity of a system can be understood as a measure for the number of components and their interactions. However, there is no uniform definition of system complexity. Hence, this publication estimates the complexity of the eHEPP configuration C_{sys} by the sum of the failure rates of its constituting components. Thus, the complexity of an eHEPP configuration

(2) $\quad C_{sys} = \lambda_{pipe} + \lambda_{elec} + \lambda_{eHEPP}$

is represented by the sum of the failure rates of the pipe system, the electric system and the eHEPP unit(s). The length-dependent failure rate of the pipe system, λ_{pipe}, is estimated by scaling the failure rate

$\lambda_{pipe,ref}$ of a reference hydraulic pipe system with the total fluid volume

$$(3) \quad \lambda_{pipe} = \lambda_{pipe,ref} \cdot \frac{V_{fl}}{V_{fl,ref}}.$$

System Availability

The availability A_{sys} of the eHEPP configurations on system level is estimated by the dispatch reliability of the system. It is assumed for all configurations that the aircraft is allowed to be operated for a certain time (risk time) with reduced internal redundancy, for instance the loss of one EMP or MCE. The loss of the entire eHEPP is considered as NO GO item in the MMEL while a dispatch (GO IF) is permitted, as long as one EMP mode is available (see TABLE 2).

TABLE 2: Dispatch Conditions

Function	Loss of Redundant Path	Loss of eHEPP
NLG (ext. and retr.)	GO IF	NO GO
NLG (steering)	GO IF	NO GO
MLG (ext. and retr.)	GO IF	NO GO
F/C	GO IF	NO GO

4.2. System Mass

The system mass of an eHEPP configuration composes of the mass of the hydraulic pipe system m_{pipe}, the mass of the eHEPP units m_{eHEPP}, and the induced electric and communication cable masses m_{cable}

$$(4) \quad m_{sys} = m_{pipe} + m_{eHEPP} + m_{cable}.$$

The determination of the system mass is based on a sizing of the eHEPP and the pipe system. For this study a dedicated sizing method was developed, based on the approach described by DUNKER throughout [18], [7], [19], and [4] that uses a steady state model of the hydraulic system.

System Definition and Construction

In the first step of the sizing a mathematical description of the pipe system is created. Under the assumption that hydraulic fluid only flows in one direction it can be modeled as directed graph (digraph). The high and low pressure system are represented by separate digraphs. The edges of the digraph define pipes. Nodes represent junctions in the pipe system. The pump of the system is always assumed to be connected to the source node of the digraph while the consumers are connected to the end nodes. A digraph can be described by an incidence matrix A,

which defines the relation between nodes and edges. The incidence matrix is used to calculate the flow distribution q in the pipe system by solving

$$(5) \quad b = A \cdot q$$

where b denotes the external flow vector that describes external flows into and out of the system (e.g. at the consumer nodes). It is derived from the hydraulic load analysis (see next step). In addition the digraph can be described by its adjacency matrix B that specifies which nodes are connected to each other by an edge. The adjacency matrix is used to calculate the pressure distribution in the system

$$(6) \quad (E + B) \cdot p + \Delta p_{loss} = h$$

where the node pressure vector p represents the pressures in the nodes, Δp_{loss} represents the pressure losses in the pipe sections, h defines external pressures like the pump and reservoir reference pressures, and E is the identity matrix.

Hydraulic Load Analysis

The hydraulic load analysis determines the maximum steady state consumer flow demands under sizing flight conditions (e.g. one engine inoperative). The flow demand of a flight control actuator is modelled via

$$(7) \quad Q_{F/C} = k_{F/C} \cdot \dot{\delta}_{F/C}$$

with the linear flow factor $k_{F/C}$ that represents the size and lever of the actuator [18]. The deflection rates $\dot{\delta}_{F/C}$ are derived from handling qualities. It is important to distinguish sizing flight conditions and flight phases. Flight phases (of a mission, see section 4.3) are time dependent and evaluated for the determination of the average performance. The sizing conditions represent the maximum load cases and are time independent. From the flow distribution q the maximum required pump flow rate $Q_{p,max}$ can be determined and via

$$(8) \quad V_{th} = \frac{Q_{p,max}}{n_{max} \cdot \eta_{vol}(n_{max})}$$

the required pump displacement is sized.

Pre-Processing

Different parameters are pre-calculated to reduce computation effort of the following optimization run [7].

First the pressure losses

$$(9) \quad \Delta p_{loss} = \frac{1}{2} \cdot \rho(v_{fl}) \cdot v_i^2 \cdot \left(\lambda \cdot \frac{l}{d} + \xi\right)$$

can be calculated in all pipe sections and for all available diameter sizes based on the flow distribution in the system. The resistance of the straight pipe segments is represented by the coefficient λ and the additional line resistance of bends etc. is modeled by ξ. For the calculation of the losses a conservative fluid temperature of $v_{fl} = -15°C$ is applied [20] (see TABLE 3). In the same way the masses of the pipe sections can be pre-calculated for all available pipe diameters. The mass of the i-th section

$$(10) \quad m_{pipe,i} = m_{dry,i} + m_{cl,i} + m_{fit,i} + m_{fl,i} = f(d_i, l_i)$$

is formed by the dry mass of the pipe $m_{dry,i}$, the mass of clamps $m_{cl,i}$, fittings $m_{fit,i}$ and the mass of the fluid $m_{fl,i}$, being a function of the inner diameter d_i and the pipe length l_i. The pipe lengths of the sections are known from the definition of the (pipe) system topology in section 2.4.

Sizing and Optimization of the Pipe System The sizing of the pipe system is defined as a discrete optimization problem (discrete dash sizes) [7]. The objective is to find the diameter set that minimizes the pipe system mass. A genetic algorithm is applied to solve the problem. The individuals are represented by sets of pipe diameters while groups of several individuals form a population. The fitness of an individual is expressed by the pipe system mass

$$(11) \quad m_{pipe} = \sum_{i=1}^{m} m_{pipe,i}$$

being is the sum of the masses of all sections. The sizing, respectively the optimization is bounded by two important constraints (compare [7]). First, a minimum delta pressure Δp_{min} at the actuators must be ensured. The actuator delta pressures are obtained from the pressure distribution. Second, the fluid velocity must not exceed a specified limit $v_{fl,max}$. The requirements are defined in TABLE 3. The result of the optimization is a final set of diameters of the high and low pressure pipe system as well as the corresponding (minimum) pipe system mass.

Post-Processing

In the post-processing the eHEPP mass and the induced electric and communication system masses are determined. The eHEPP mass is composed of

TABLE 3: Sizing Parameters and Constraints

Symbol	Description	Unit	Value	Ref.
p_0	Reservoir Pressure	[bar]	3.5	-
Δp_{min}	Minimum actuator delta pressure	[bar]	165	[20]
$v_{fl,max,HP}$	Max. HP fluid velocity	[m/s]	10	[21]
$v_{fl,max,LP}$	Max. LP fluid velocity	[m/s]	5	[21]
n_{max}	Max. EMP speed	[1/min]	10,000	-
v_{fl}	Fluid temp.	[°C]	−15	[20]
η_{ADGB}	Efficiency of ADGB	[-]	0.95	-
η_{VFG}	Efficiency of VFG	[-]	0.90	-
η_{ATRU}	Efficiency of ATRU	[-]	0.93	-
$\eta_{vol}(n_{max})$	Volumetric efficiency at max. speed	[-]	0.98	-
$\eta_{hm}(n_{max})$	Hydro-mechanical efficiency at max. speed	[-]	0.66	-

the sum of its sub-component masses

$$(12) \quad \begin{aligned} m_{eHEPP} &= z_{MCE} \cdot m_{MCE} \\ &+ z_{mot} \cdot (m_{mot} + m_{mot,cool}) \\ &+ z_{pump} \cdot m_{pump} \\ &+ m_{rsvr} + m_{sens} + m_{accu} \\ &+ m_{valve} + m_{frame} \end{aligned}$$

Note that redundancies are taken into account by multiplying the component mass by the number z of installed units in the pack. For the estimation of the mass of the pump

$$(13) \quad m_{pump} = k_{pump} \cdot V_{th}$$

a linear scaling approach is applied. The factor k_{pump} was derived from the relation between mass and displacement volume of several industrial IGPs. It can be assumed that pumps, which are optimized for aerospace applications, would be lighter so that this is a conservative estimation. The electric motor is sized using the maximum steady state motor torque $T_{mot,max}$

$$(14) \quad m_{mot} = k_{mot} \cdot T_{mot,max}.$$

It is represented by the maximum hydraulic torque of the pump

$$(15) \quad T_{mot,max} = T_{hyd,max} = \frac{V_{th} \cdot \Delta p}{2 \cdot \pi \cdot \eta_{hm}(n_{max})}$$

that is calculated from the pump displacement, the delta pressure and the hydro-mechanical efficiency at maximum EMP speed $\eta_{hm}(n_{max})$. This approach obviously neglects the dynamic torque for the acceleration of the EMP, which is required for a fast response of the pressure controller. But since the dynamic requirements for aerospace pumps specified by SAE Aerospace Standard 595 [22] are very strict (response times of $50-100\mathrm{ms}$), a high additional torque would be necessary, leading to relatively large motor sizes. Here future studies will have to investigate smart (control and system) concepts that minimize the required dynamic motor torque. Further, it will have to be clarified, whether the requirements of SAE AS 595 could be relaxed for VSFD EMP concepts in certain (local) applications. However, for this study the steady state motor sizing is assumed to be sufficiently accurate to allow for a qualitative (relative) comparison of eHEPP sizings.

The mass of the hydraulic jacket cooling of the motor is sized by scaling a reference mass with the maximum electrical power demand of the motor

$$(16) \quad m_{cool} = k_{cool} \cdot P_{mot,max}.$$

The maximum motor input power is derived via

$$(17) \quad P_{mot,max} = \frac{Q_{p,max} \cdot \Delta p}{\eta_{hm} \cdot \eta_{vol} \cdot \eta_{mot}}.$$

The mass of the MCE is sized via a linear scaling approach

$$(18) \quad m_{MCE} = k_{MCE} \cdot P_{MCE,max}$$

based on the electrical MCE input power where the factor k_{MCE} depends on the place of installation of the MCE. Specifically, on the cooling concept. The maximum electrical input power is derived from the motor input power via

$$(19) \quad P_{MCE,max} = \frac{P_{mot,max}}{\eta_{MCE}}.$$

The total mass of the reservoir is the sum of the dry mass and the mass of the fluid. The dry mass of the reservoir

$$(20) \quad m_{rsvr} = k_{rsvr} \cdot V_{rsvr} + m_{rsvr,0}$$

is determined with a scaling law based on the reservoir capacity V_{rsvr}. The capacity is determined according to SAE AS 5586 [23]. The reservoir compensates the variation of the systems fluid volume during operation, for example

- when the temperature varies ΔV_θ,
- when differential actuators are moved $\Delta V_{diff,act}$, or
- when the pressure level changes ΔV_p.

The required reservoir capacity

$$(21) \quad V_{rsvr} = V_{rsvr,0} + \Delta V_\theta + \Delta V_{diff,act} + \Delta V_p$$

is obtained from the sum of these variations plus a fixed volume $V_{rsvr,0}$. For the sizing the maximum delta volume over all operating conditions has to be determined. The sizing of the remaining eHEPP components such as sensors and valves uses similar scaling approaches and is therefore skipped here.

Power and Communication Cable Masses
The induced electrical mass by additional electric power cables is calculated via

$$(22) \quad m_{cable,elec} = k_{cable,elec} \cdot l_{cable,elec}$$

where $l_{cable,elec}$ represents the length of the additional power cables and $k_{cable,elec}$ is the specific mass of the power cable. In the same way the induced mass in the communication system, caused by extension of the AFDX network, is estimated via

$$(23) \quad m_{cable,AFDX} = k_{cable,AFDX} \cdot l_{cable,AFDX}$$

where $l_{cable,AFDX}$ is the length of the additional communication bus routes and $k_{cable,AFDX}$ is the specific mass of the AFDX cable. The total induced cable mass is

$$(24) \quad m_{cable} = m_{cable,elec} + m_{cable,AFDX}.$$

4.3. Secondary Power Consumption

For the sized eHEPP system the average secondary power consumption at the engine shaft is determined based on the 800nm reference flight mission shown in FIGURE 7. The hydraulic load profile has the typical characteristic with a few load peaks, during extension and retraction of the landing gear, and rel-
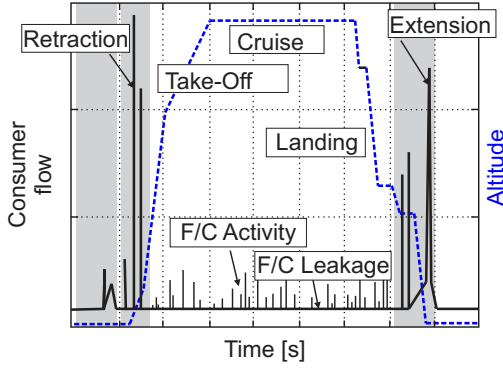
FIGURE 7: Qualitative Hydraulic Load Profile in Reference Mission

FIGURE 8: System Mass

atively low flow consumption of the F/C most of the time. The mission consists of the phases: ground operation (taxi out), take-off and climb, cruise, descent and approach, landing and finally taxi in. Two modes of operation are considered in the analysis:

- **Back-up mode:** The F/C SCUs are passive so that eHEPP only provides F/C leakage and regular landing gear supply.

- **Active mode:** eHEPP supplies the flow demand of the active F/C SCUs and the landing gear.

The average power consumption of the entire eHEPP system configuration in a mission with the duration $\Delta t_{mission}$ is formed by

$$(25) \quad P_{eng,av} = \frac{1}{\Delta t_{mission}} \cdot \left(\sum_{i=1}^{m} \sum_{j=1}^{n} P_{eng,av,eHEPP,i,j} \cdot \Delta t_j \right)$$

the summation of the energy consumption of the i-th eHEPP in the j-th flight phase with the duration Δt_j. The average power consumption of the i-th eHEPP

$$(26) \quad P_{eng,av,eHEPP,i,j} = \frac{Q_{av,eHEPP,i,j} \cdot \Delta p}{\eta_{VFG} \cdot \eta_{ATRU} \cdot \eta_{ADGB} \cdot \eta_{eHEPP,i,j}}$$

is derived from the average hydraulic load $Q_{av,eHEPP,i,j}$ where the simplifying assumption of an ideally constant delta pressure of $\Delta p = 206\,\mathrm{bar}$ was made. The average hydraulic flow rate is determined per flight phase and depends on the consumers allocated to the i-th eHEPP. For simplicity the efficiencies of generator η_{VFG}, ATRU η_{ATRU}, and accessory driven gear box (ADGB) η_{ADGB} are assumed constant over the range of operation because they are not part of the sizing. The efficiency of the eHEPP

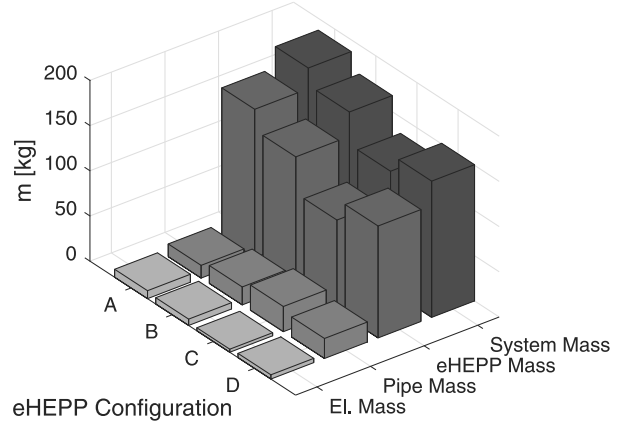$$(27) \quad \eta_{eHEPP,i,j} = \frac{1}{\eta_{MCE} \cdot \eta_{mot} \cdot \eta_{hm,av} \cdot \eta_{vol,av}},$$

specifically, the efficiencies of MCE, motor, and pump depend on the operating point (EMP speed).

5. SYSTEM KEY PERFORMANCE EVALUATION

The resulting key performance of the eHEPP configurations is evaluated in the following.

System Mass
FIGURE 8 presents the resulting system masses (dark grey) as well as the masses of the sub-systems (lighter shades of grey). The highest system mass of about $187\,\mathrm{kg}$ is obtained for the distributed configuration A. The eHEPP mass (three eHEPPs) of this configuration is $164\,\mathrm{kg}$, which is $88\,\%$ of the total mass. This shows clearly that the main contribution to the mass comes from the eH supply modules, particularly from the integrated electric motors and MCEs. Even though the pipe system mass of the distributed configuration shows the expected weight savings ($14\,\mathrm{kg}$ vs. $27\,\mathrm{kg}$ of the central system) they cannot outweigh the additional mass of multiple eHEPPs.

Accordingly, with a weight of $132\,\mathrm{kg}$ the central configuration C is the lightest system. This is mainly because the mass of the central eHEPP ($101\,\mathrm{kg}$) is lighter by almost $63\,\mathrm{kg}$ compared to the distributed configuration (A). But again it is the largest proportion of the system mass ($76\,\%$). The system masses of configurations B and D lie between A and C. All configurations have in common that the masses of additional power and communication cables generate the lowest contribution to the system mass.

Secondary Power Offtakes
Two operating modes were considered: active and back-up, compare section 4.3. The average secondary power offtake from the engine of the eHEPP configurations in both modes are shown in FIGURE 9. The active mode consumes twice as much power as the back-up mode. This is because the operating
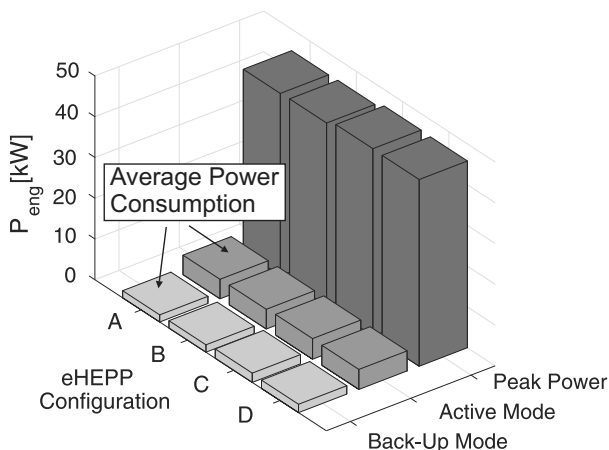
FIGURE 9: Secondary Power Consumption

FIGURE 10: System Complexity and Availability

times of the landing gear are short (a few seconds) so that the dominant contribution to power consumption comes from the F/C activity (leakage vs. active operation). Configuration C consumes the most power in both operating modes. This implies that configuration C operates at the poorest (relative) efficiency. This is mainly due to two reasons. Firstly, the EMP of configuration C has the largest size of all EMPs so that the relative load and thus the efficiency is lower (compare FIGURE 5). Secondly, all other configurations feature at least one eHEPP that only supplies the landing gear and can be switched off during the rest of the flight. This means zero energy consumption during that time. However, in general the delta in power consumption between the configurations is very low ($<0.5\,\mathrm{kW}$) in both modes so that in terms of efficiency no clear advantage of any configuration could be observed. Next to the average power consumption the maximum, or peak power offtake is shown. It can be seen that it is quite similar for all configurations. This corresponds to the above results for average power consumption. The peak power demand is many times higher than the average power demand, which points out that the eHEPPs are extremely oversized for normal operation.

System Availability, Complexity and Safety
The assumptions described in section 4.1 lead to equal safety (reliability) in the considered F/C top events for all configurations (see equation 1). It was shown that the required reliability of $F \leq 1 \cdot 10^{-9}$ /FH is reached for all top events and therefore does not serve as distinctive criterion.

System complexity (dark grey) and availability (light grey) are shown in FIGURE 10. They are normalized to the highest availability and to the highest complexity, respectively. The central configuration C achieves the best availability because there is only one eHEPP
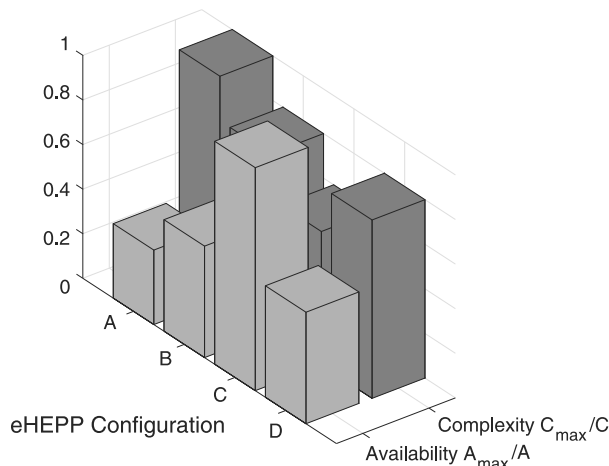
unit that can possibly cause a NO GO event while in any other configuration two or three eHEPP units have to be considered increasing the probability of a NO GO. The system complexity is directly related to the availability since in a more complex configuration there are more components/functions that could possibly fail. Accordingly, configuration C is the least complex system. Obviously, the shorter pipe system of the distributed configuration is not balancing out this impact. Yet, this result is based on very rough assumptions regarding the failure rate of the pipe system. Moreover, it neglects failures in the electrical distribution network.

Comparison
For a final and overall comparison all results are summarized in normalized form in FIGURE 11.
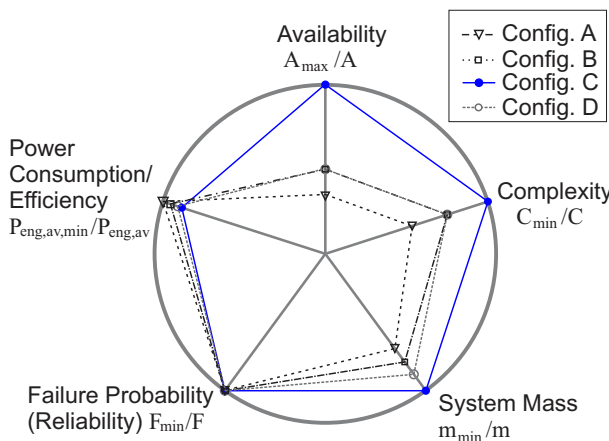

FIGURE 11: RADVIZ-Diagram of the Configurations

The plot underlines the advantageous design of configuration C in almost any attribute, except the efficiency. However, as mentioned above, the system efficiencies differ only slightly. Apparently even the large centralized EMPs of configuration C operate at

a good average efficiency. This is mainly due to the high part load efficiency of the EMP concept with IGP. As in particular the mass savings with configuration C are significant it appears as clear favorite of the study. It is expected that the mass saving would outweigh the slightly reduced efficiency. However, this must be proven in a mission analysis that includes the evaluation of direct operating cost. An obvious drawback of configuration C is a higher hydraulic installation effort since a central pipe line from the front to the empennage is needed. This results in a basic trade-off between a lower system mass and reduced installation effort. This needs to be assessed by aircraft manufacturers based on their needs and constraints of the FAL.

6. CONCLUSION AND OUTLOOK

In future MEA system architectures with central electric distribution networks eH systems can represent the enabling (bridge) technology by supplying conventional hydraulic actuators where PbW actuation lacks maturity or is disadvantageous. For a MEA architecture concept with an E-Wing this study investigates the application of eHEPPs for the eH supply of the empennage F/C functions and the landing gear. A VSFD EMP with IGP is applied to achieve high efficiencies. Two fully redundant EMPs in the package ensure a high operational availability. Based on a steady state system sizing, the study reveals that a system configuration with one centralized eHEPP supplying all consumers has the lowest system mass. Even though a distributed configuration with multiple local eHEPPs leads to the expected savings in pipe system mass, this cannot balance out the high mass of additional electric equipment. In terms of power consumption no significant delta between the configuration are observed. The new EMP concept offers a good efficiency over a wide range of operation leading to similar efficiency of all eHEPPs. A safety analysis shows that the common safety requirement for an extremely improbable loss of the F/C actuation functions can be met for all configurations. Last but not least a centralized eHEPP with redundant EMPs, allowing to dispatch also if one EMP or MCE fails, improves the operational availability of the eH supply since there are less eHEPPs that can cause a NO GO event.

It can be noted as general result of this evaluation that in eH systems with quite heavy electric equipment the main contribution to the system mass shifts from the conduction (pipe system) to the generation components, compared to conventional hydraulic systems with EDPs. As a consequence, also the priorities in design shift from pipe system optimization towards low weight EMP sizing. This is true for both, the central and the distributed configurations. A reduction of the eHEPP mass appears possible if sizing peak loads can be reduced. Moreover, eH systems with fewer consumers allow to design EMPs closer to the specific load characteristics of the consumers. Future activities have to develop eHEPP systems and control concepts that optimize the design. Further, thermal investigations of eH systems need to be conducted. Smaller hydraulic systems have a reduced pipe system surface for cooling while extra heat input into the system is expected from the electric equipment. Moreover, eHEPPs that are not permanently in operation (e.g. for NLG supply) cool down during flight. This will also have to be considered.

CONTACT INFORMATION
Nils Trochelmann
Hamburg University of Technology
Institute of Aircraft Systems Engineering
Neßpriel 5, 21129, Hamburg, Germany
nils.trochelmann@tuhh.de

REFERENCES

[1] Rosero, J.A., E. Ortega, E. Aldabas, and L. Romeral: *Moving Towards a More Electric Aircraft*. In *IEEE AE Systems Magazine*, 2007.

[2] Maré, J. C. and J. Fu: *Review on signal-by-wire and power-by-wire actuation for more electric aircraft*. In *Chinese Journal of Aeronautics (CJA)*, March 2017.

[3] Fervel, M., L. Andrieu, M. Todeschi, and J. Roizes: *More Electrical Aircraft Control*. In *Proceedings of the 6th International Conference on Recent Advances in Aerospace Actuation Systems and Components (R3ASC)*, Toulouse, France, 2014.

[4] Dunker, C., R. Bornholdt, F. Thielecke, and R.M. Behr: *Architecture and Parameter Optimization for Aircraft Electro-Hydraulic Power Generation and Distribution Systems*. In *SAE Aerotech Congress & Exhibition*, Seattle, USA, September 2015. SAE International.

[5] Todeschi, M.: *Airbus - EMAs for flight control actuation system 2012 status and perspectives*. In *Proceedings of the 5th international conference on recent advances in aerospace actuation systems and components (R3ASC)*, Toulouse, France, 2012.

[6] Van den Bossche, D.: *The A380 Flight Control Electrohydrostatic Actuators, Achievements and Lessons Learnt*. In *Proceedings of the 25th International Congress on of the Aeronautical Sciences (ICAS)*, Hamburg, Germany, 2006.

[7] Dunker, C., F. Thielecke, and T. Hohmann: *Optimal Sizing of Pipe Networks in Aircraft Hydraulic System Preliminary Design*. In *Bath/ASME Symposium on Fluid Power and Motion Control (FPMC)*, Bath, UK, September 2012. Deutsche Gesellschaft für Luft- und Raumfahrt.

[8] Aigner, B., F. Peter, E. Stumpf, B. Hauber, and D. Metzler: *Assessment of electromechanical Flight Control Actuators with Regard to direct Operating Costs*. In *Deutscher Luft- und Raumfahrtkongress (DLRK) 2016*, Braunschweig, September 2016. Deutsche Gesellschaft für Luft- und Raumfahrt.

[9] Schubert, H.-J.: *Advanced Technologies Demonstrator (ATD) Entwicklung und Erprobung einer Elektronischen Flugsteuerung (Fly-By-Wire, EFCS) der 2. Generation*. In *DGLR Vortragsreihe*, Hamburg, 2000.

[10] Doberstein, D.: *Modellbasierter Entwurf und experimentelle Validierung von elektromechanischen Betätigungsfunktionen für ein Bugfahrwerksystem*. PhD thesis, TUHH, 2016.

[11] Elliot, N., S. Linforth, and C. Moore: *Thermae II (Main Landing Gear Door EH Actuation System) Integration and Testing*. In *Proceedings of the 7th International Conference on Recent Advances in Aerospace Actuation Systems and Components (R3ASC)*, Toulouse, France, 2016.

[12] Greißner, C.: *Konzeption und experimentelle Untersuchung geregelter Bugfahrwerksfunktionen durch ein elektrohydraulisches Versorgungsmodul*. PhD thesis, TUHH, 2008.

[13] Kirchmann, I., U. Grabherr, M. Gitterle, and M. Hornung: *Elektro-Hydraulische Antriebe Am Flugzeugfahrwerk*. In *Deutscher Luft- und Raumfahrtkongress (DLRK) 2015*, Rostock, Germany, September 2015. Deutsche Gesellschaft für Luft- und Raumfahrt.

[14] Dunker, C., K. Poole, and F. Thielecke: *Towards More-Efficient Aircraft Hydraulic Systems: Conceptual Design of a Variable-Speed Fixed Displacement Electric Motor Pump*. In *SAE Aerotech Congress Exhibition*, Montreal, Canada, September 2013. SAE International.

[15] Neubert, T.: *Untersuchung von drehzahlveränderbaren Pumpen*. PhD thesis, TU Dresden, 2001.

[16] Rühlicke, I.: *Elektrohydraulische Antriebssysteme mit drehzahlveränderbarer Pumpe*. PhD thesis, TU Dresden, 1997.

[17] Vahl, A.: *Interaktive Zuverlässigkeitsanalyse von Flugzeug-Systemarchitekturen*. PhD thesis, TUHH, 1998.

[18] Dunker, C., F. Thielecke, and T. Hohmann: *New Computer Aided Methods for Preliminary Architecting and Sizing of Aircraft Hydraulic Systems*. In *Deutscher Luft- und Raumfahrtkongress (DLRK) 2011*, Bremen, September 2011. Deutsche Gesellschaft für Luft- und Raumfahrt.

[19] Dunker, C., F. Thielecke, and T. Hohmann: *Analysis of Minimum Delta Pressure Specifications Between Actuators and Hydraulic Power Generation and their Effect on Overall System Sizing*. In *Proceedings of the 6th International Conference on Recent Advances in Aerospace Actuation Systems and Components (R3ASC)*, Toulouse, April 2014.

[20] Behr, R.M. and V. Baumbach: *Aircraft Hydraulic Thermal Control*. In *Proceedings of the 2nd International Workshop on Aircraft System Technologies*, Hamburg, 2009.

[21] Callenere, M. and G. Sauterey: *Fluid Velocity Limits in Hydraulic Systems: Detrimental Effects on Distribution Systems*. In *Proceedings of the 2nd International Conference on Recent Advances in Aerospace Actuation Systems and Components (R3ASC)*, Toulouse, France, 2004.

[22] SAE International (Publ.): *Aerospace Standard 595 - Pressure Compensated variable displacement aircraft pumps - Revision D*. 2010.

[23] SAE International (Publ.): *Aerospace Standard 5586 - General Requirements for Hydraulic System Reservoirs*. 2005.